J HK Coll Radiol 2002;5:19-23

ORIGINAL ARTICLE

Scattered Radiation Level During Computed Tomography Fluoroscopy

CB Chan, LK Chan, HS Lam

Department of Radiology, Kwong Wah Hospital, Kowloon, Hong Kong

ABSTRACT

Objective: *To assess the scattered radiation dose to personnel during CT fluoroscopy using phantom measurements.*
Materials and Methods: *Scattered radiation levels (normalised by mA and scan time) were measured at different distances from the isocentre of the CT scanner with different kV settings and slice thicknesses using supplied head and body phantoms in three configurations (head front side and back side; body front side). The effect of varying the phantom effective thickness on scattered radiation dose was also evaluated using a plain phantom.*
Results: *For each configuration, the scattered radiation dose at each applied tube potential was linearly related to the distance from the isocentre when the slice thickness and phantom effective thickness were constant. In the body front side configuration (the only one tested), doubling the slice thickness approximately doubled the scattered radiation level. The scattered radiation dose at each kV setting was also linearly related to the phantom effective thickness when the distance from the isocentre and slice thickness were fixed.*
Conclusion: *The results of this study (in the form of the linear equations obtained) enable the scattered radiation dose to be estimated based on the distance from the isocentre and kV setting of a particular CT scanner and scanning configuration, and can be used to develop guidelines for radiation protection management.*

Key Words: *Computed tomography, Fluoroscopy, Radiation protection, Scattering, radiation*

INTRODUCTION

CT has been adopted for interventional procedures for many years.[1-2] Although a lack of real-time imaging information limited the popularity of conventional (non-fluoroscopic) CT as a biopsy localisation procedure compared with ultrasonography and fluoroscopy, this situation changed in the early 1990s with the advent of fluoroscopic CT, which enables real-time images to be reconstructed and displayed.[3-4] Real-time CT scanning offers many advantages to radiologists, such as immediate feedback of images, improvement of lesion targeting, and reduced procedure times. CT fluoroscopy has been used to guide intracranial, chest, abdominal, and pelvic biopsy procedures, as well as for fluid collection drainage.[5-8]

A major consideration when using CT fluoroscopy is that personnel are required to be in the scanning room while the x-ray exposure occurs. Personnel exposure rates due to scattered radiation could be high at locations near the scanning plane. The purpose of the present study, therefore, was to assess the scattered radiation level during CT fluoroscopy by means of phantom measurements. Taking into account the 'as low as reasonably achievable' (ALARA) principle and the annual occupational dose limit, the results of our study can be used to develop guidelines for exposure time during CT fluoroscopy. However, it is important to note that these guidelines are specific for a particular scanner and scanning configurations used during CT fluoroscopic interventional procedures.

MATERIALS AND METHODS

The CT scanner used was a third generation Xpress/SX (Toshiba, Tokyo, Japan) equipped with a real-time reconstruction system (TSXF-001B) for performing image reconstruction and display during continuous scanning. During acceptance testing of the X-ray tube, the half value layer was found to be 5.85 mm Al at 100 kV. The CT dose index was measured to be 21.5 mGy per 100 mA at 120 kV with 7 mm slice thickness at 1 cm interior to the surface of the 16 cm

Correspondence: *Dr. CB Chan, Department of Radiology, Kwong Wah Hospital, 25 Waterloo Road, Kowloon, Hong Kong.*
Tel: (852) 2710 8514; Fax: (852) 2781 5452;
E-mail: chancb@ha.org.hk

Submitted: 22 August 2001; Accepted: 26 November 2001.

diameter head dosimetry phantom and 6.7 mGy per 100 mA at 120 kV with 5 mm slice thickness at 1 cm interior to the surface of the 32 cm diameter body dosimetry phantom.[9]

Made of perspex and filled with water, a 25 cm diameter/ 9 cm thickness head phantom and a 33 cm diameter/ 10.5 cm thickness body phantom supplied with the CT scanner were used, and scattered radiation dose values were measured along the midline at around 30 to 70 cm from the isocentre of the scanner using a Radcal radiation monitor model 9010. Measurements were made at two positions, namely in front of the scanner (front side) and at the back of the scanner (back side), for the head phantom, and one position, namely front side, for the body phantom. Since the scattered radiation dose is proportional to the X-ray tube current and scanning time for a constant X-ray tube potential and slice thickness, the scattered radiation dose values at different distances from the isocentre were measured at 100, 120, and 135 kV with a fixed 50 mA tube current, 20 second scanning time, and 5 mm slice thickness. For the body phantom case, the scattered radiation dose values with a constant 10 mm slice thickness were also measured.

Additionally, the attenuation of scattered radiation dose values due to the effective thickness of the phantom (i.e. the thickness measured from the scanning plane to the circular end of the phantom) was investigated using a plain 14 cm diameter phantom made of perspex and filled with water. In this protocol, the tube potential and current were fixed, as was the slice thickness, while the phantom effective thickness was varied between 4 cm and 20 cm. The ensuing scattered radiation dose values were measured along the midline of the scanner at a fixed distance of 40.8 cm from the isocentre.

Data collected as described above were analysed by linear regression and correlation analyses.[10]

RESULTS

At a fixed (head = 5.5 cm; body = 7 cm) phantom effective thickness, and a constant (5 mm) slice thickness, the ln-ln (natural log) relationship between the scattered radiation dose and the distance from the isocentre was linear at each tube potential applied in all three of the configurations adopted. Accordingly, one linear equation for each kV setting of each configuration can be obtained in the following form:

$$\ln(y) = m_1 \bullet \ln(x) + c_1 , \qquad (1)$$

where y is the scattered radiation dose (in μSv/mA), x is the distance from the isocentre (in cm), and m_1 is the slope and c_1 is the y-intercept of the linear equation. With suitable mathematical manipulation, equation (1) can also be expressed as:

$$y = e^{c_1} \bullet x^{m_1} . \qquad (2)$$

Table 1 lists the values of m_1, c_1, and the correlation coefficient (r) for each linear equation, i.e. for each kV setting of each configuration.

This table shows that the values of m_1 remain nearly the same for the different kV settings, while those of c_1 increase with increasing applied tube potential. In fact, a linear relationship was found between c_1 and the kV setting at each configuration. Hence, one linear equation for each configuration can be obtained in the following form:

$$c_1 = m_2 \bullet kV + c_2 , \qquad (3)$$

where m_2 is the slope and c_2 is the y-intercept of the linear equation. Table 2 lists the values of m_2, c_2, and r for each linear equation.

Substituting equation (3) into equation (2) gives:

$$y = e^{(m_2 \bullet kV + c_2)} \bullet x^{m_1} . \qquad (4)$$

Table 1. Slope (m_1), y-intercept (c_1), and correlation coefficient (r) characteristics of the linear equations in ln-ln scale found between the scattered radiation dose and distance from the isocentre of the scanner for each kV setting of each configuration.

Configuration	kV	m_1	c_1	r
Head (front side)	100	-1.93	4.39	1.00
	120	-1.95	4.98	1.00
	135	-1.96	5.36	1.00
Head (back side)	100	-2.17	5.20	1.00
	120	-2.10	5.47	1.00
	135	-2.14	5.99	1.00
Body (front side)	100	-1.82	3.77	1.00
	120	-1.93	4.79	1.00
	135	-1.94	5.18	1.00

Table 2. Slope (m_2), y-intercept (c_2), and correlation coefficient (r) of the linear equations found between c_1 and the kV setting at each configuration.

Configuration	m_2	c_2	r
Head (front side)	0.028	1.63	1.00
Head (back side)	0.022	2.95	0.96
Body (front side)	0.041	-0.25	0.99

Table 3. Summary of parameters of the equation for estimating scattered radiation dose based on the distance from the isocentre of the scanner and kV setting at particular (known) mA and constant (5 mm) slice thickness at each configuration.

Configuration	m_1	m_2	c_2
Head (front side)	-1.95	0.028	1.63
Head (back side)	-2.14	0.022	2.95
Body (front side)	-1.90	0.041	-0.25

For each configuration, then, equation (4) provides a means of estimating the scattered radiation dose based on the distance from the isocentre and applied tube potential, allowing for a (known) mA, a fixed (head = 5.5 cm; body = 7 cm) phantom effective thickness, and a constant (5 mm) slice thickness. The m_1 in equation (4) can be taken as the mean of the m_1's in each configuration in Table 1. The validity of equation (4) depends on the reliability of m_1's and c_1's derived from the linear regression, which, in our case, is very high indeed based on the good r values (1 or very close to 1) in Tables 1 and 2. Table 3 summarises the parameters of equation (4) for each configuration.

Figure 1 shows plots of the estimated scattered radiation dose versus distance from the isocentre at 120 kV, 50 mA, 200 seconds (a typical total scan time duration for a CT interventional procedure), a fixed (head = 5.5 cm; body = 7 cm) phantom effective thickness, and a constant (5 mm) slice thickness for all three configurations.

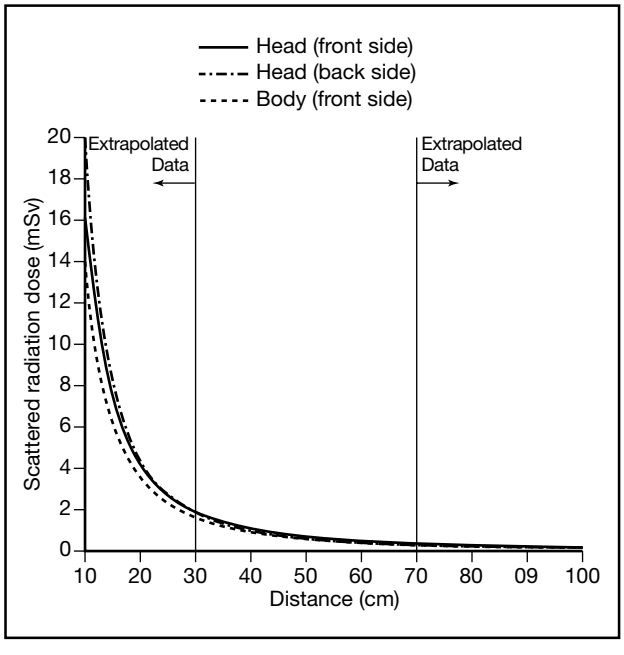

Figure 1. Plots of the scattered radiation dose versus distance from the isocentre of the scanner at 120 kV, 50 mA, 200-second scan time, fixed (head = 5.5 cm; body = 7 cm) phantom effective thickness, and constant (5 mm) slice thickness for the three configurations adopted.

Table 4. Parameters of the equation for estimating scattered radiation dose based on the distance from the isocentre of the scanner and kV setting (and known mA) for the body front side configuration with 5 mm and 10 mm slice thicknesses.

Slice thickness (mm)	m_1	m_2	c_2
5	-1.90	0.041	-0.25
10	-1.92	0.025	2.38

The scattered radiation dose depends not only on the applied tube potential and current, but also on the slice thickness, phantom diameter, and phantom effective thickness. Table 4 lists the parameters of equation (4) for the body front side configuration with 5 mm and 10 mm slice thicknesses, while the corresponding plots at 120 kV, 50 mA, 200 second scan time, and phantom effective thickness of 7 cm are shown in Figure 2. Using these study parameters, the scattered radiation dose values for the 10 mm slice thickness were found to be roughly double those of the 5 mm slice thickness.

The present results (e.g. in Figure 1) showed that the scattered radiation dose values due to a smaller phantom diameter (i.e. the head phantom) were greater than those due to a larger phantom diameter (i.e. the body phantom), although in general it should be to the contrary. However, it should be stressed that the effective thickness of the head phantom (5.5 cm) is smaller than that of the body phantom (7 cm). It is most likely that the larger scattered radiation dose values due to the body phantom are attenuated by its larger effective

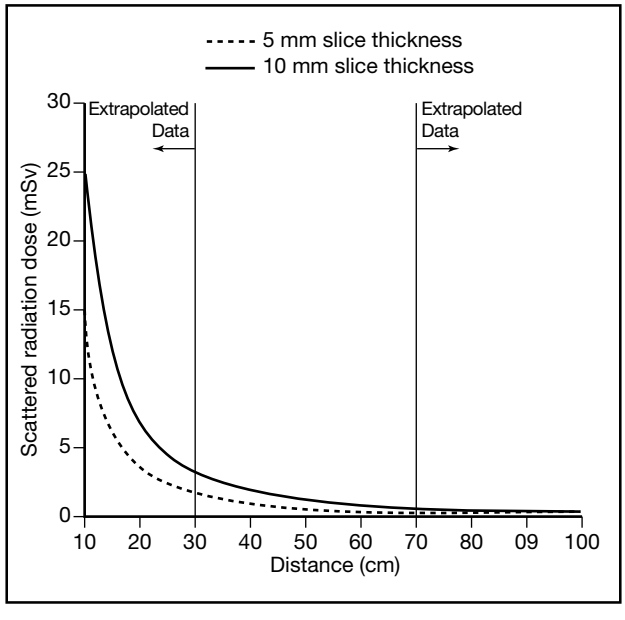

Figure 2. Plots of the scattered radiation dose versus the distance from the isocentre of the scanner at 120 kV, 50 mA, 200-second scan time, fixed (7 cm) phantom effective thickness, and constant 5 mm or 10 mm slice thicknesses for the body front side configuration.

thickness, resulting in lower scattered radiation dose values than those due to the head phantom with its smaller effective thickness.

To verify the above argument, the scattered radiation dose values at a fixed distance from the isocentre of the scanner (40.8 cm) were measured at various phantom effective thicknesses (4 to 20 cm) using the plain 14 cm diameter phantom (see Materials and Methods). At a constant 5 mm slice thickness, the semi-ln (natural log) relationship between the scattered radiation dose and phantom effective thickness was linear at each tube potential applied (100, 120, and 135 kV). Accordingly, one linear equation for each kV setting can be obtained in the following form:

$$\ln(y) = -\mu \bullet T + k , \qquad (5)$$

where T is the phantom effective thickness (in cm), and $-\mu$ is the slope and k is the y-intercept of the linear equation. With suitable mathematical manipulation, equation (5) can also be expressed as:

$$y = e^{k} \bullet e^{-\mu T} . \qquad (6)$$

Since e^{k} is a constant, a typical exponential attenuation relationship was found between the scattered radiation dose and the phantom effective thickness as follows:

$$y \propto e^{-\mu T} , \qquad (7)$$

where μ is the attenuation coefficient. Table 5 lists the values of μ of the plain phantom for the different kV settings adopted in the present study.

From equation (4), we observe that the scattered radiation dose is proportional to a power term of the distance from the isocentre, as well as an exponential term of the applied tube potential when the phantom effective thickness is fixed, i.e.:

$$y \propto e^{a_1 \cdot kV} \bullet x^{a_2} , \qquad (8)$$

where a_1 and a_2 are proportionality constants. Moreover, from equation (7), the scattered radiation dose is proportional to an exponential term of the phantom effective thickness when the distance from the isocentre and the applied kV are fixed. Hence, a more general formula for estimating the scattered radiation dose, which incorporates the attenuation effect of the phantom effective thickness, can be expressed as:

$$y = A \bullet e^{a_1 \cdot kV - \mu T} \bullet x^{a_2} , \qquad (9)$$

where A, a_1, a_2, and μ are constants that should be determined for each specific configuration under consideration.

Table 5. Attenuation coefficient (μ) of the plain phantom at different applied tube potentials.

kV	μ
100	0.051
120	0.049
135	0.046

DISCUSSION

Given the distance from the isocentre of the scanner, kV setting, tube current, and scanning time, the scattered radiation dose can be readily estimated using equation (4). The estimated dose values normally reflect the worst case scenario, as the effective thickness of patients should normally be well above that of the phantoms used in the present study. The estimated dose can thus be used as a guideline for conservative planning in radiation protection management. However, it should also be noted that the estimated dose values are specific to our scanner and scanning configurations.

To reduce the scattered radiation dose to personnel, both the ALARA principle and, more generally, that of minimising radiation dose by distance, time, and shielding should always be observed. It is evident from Figure 1 that the scattered radiation dose drops drastically at a distance of 10 to 30 cm from the isocentre of the scanner. As the scattered radiation dose is proportional to the exposure time, good management of procedure time is crucial for minimising the personnel radiation dose. In addition, personnel performing the CT fluoroscopy examination are required to wear lead collars and lead aprons as a protective measure. Minimising the energy of the X-ray source through proper choice of tube potential and current provides another means of reducing the personnel radiation dose. Furthermore, as is evident from Figure 2, slice thickness also plays an important role in the scattered radiation level during CT fluoroscopy: the thicker the slice, the greater the scattered radiation level at any given distance from the isocentre of the scanner.

CONCLUSION

The present study provided a means for estimating scattered radiation dose based on the distance from the isocentre and kV setting of a particular CT scanner and scanning configuration. The estimated dose can thus be

used as a guideline for planning in radiation protection management.

REFERENCES

1. Haaga JR, Alfidi RJ. Precise biopsy localization by computed tomography. Radiology 1976;118:603-607.
2. Mueller PR, vanSonnenberg E. Interventional radiology in the chest and abdomen. N Engl J Med 1990;322:1364-1374.
3. Katada K, Kato R, Anno H, et al. Guidance with real-time CT fluoroscopy: early clinical experience. Radiology 1996;200: 851-856.
4. Kato R, Katada K, Anno H, Suzuki S, Ida Y, Koga S. Radiation dosimetry at CT fluoroscopy: physician's hand dose and development of needle holders. Radiology 1996;201:576-578.
5. White CS, Templeton PA, Hasday JD. CT-assisted trans-bronchial needle aspiration: usefulness of CT fluoroscopy. AJR Am J Roentgenol 1998;169:393-394.
6. Meyer CA, White CS, Wu J, Futterer SF, Templeton PA. Real time CT fluoroscopy: usefulness in thoracic drainage. AJR Am J Roentgenol 1998;171:1097-1101.
7. Froelich JJ, Saar B, Hoppe M, et al. Real-time CT-fluoroscopy for guidance of percutaneous drainage procedures. J Vasc Interv Radiol 1998;9:735-740.
8. Silverman SG, Tuncali K, Adams DF, Nawfel RD, Zou KH, Judy PF. CT fluoroscopy-guided abdominal interventions: techniques, results, and radiation exposure. Radiology 1999;212:673-681.
9. Dowsett DJ, Kenny PA, Johnston RE. The physics of diagnostic imaging. London: Chapman & Hall Medical;1998:79,340.
10. Walpole RE, Myers RH, Myers SL. Probability and statistics for engineers and scientists (6th edition). New Jersey: Prentice Hall;1997:358-404.